The effect of compaction pressure, sintering time, and temperature on the characterization of an aluminum/alumina composite with rising alumina proportions

Anup Choudhury[a], Jajneswar Nanda[a*] and Sankar Narayan Das[a]

[a]Department of mechanical engineering, Siksha 'O' Anusandhan (Deemed to be University), Bhubaneswar-751030, Odisha, India

CHRONICLE	ABSTRACT
	The purpose of this article is to investigate the effect of various process parameters such as compaction pressure, sintering temperature, and time on the physio-mechanical properties of a powder metallurgy-fabricated composite made of pure aluminium/alumina. Temperatures (580°C, 600°C, and 630°C), periods (1.5, 2, and 2.5 hr), compacting loads (30KN-65KN), and alumina percentages (2, 4, 6, and 8weight percent) are all considered. X-ray diffraction (XRD) and X-ray fluorescence spectroscopy (XRF) studies are carried out to determine the phases present and their proportions. Crystallite size study is performed using XRD data, and the Al+4 weight % alumina composite has the smallest size of any composite tested. For optimization, sintering density, porosity, and microhardness are calculated. Scanning electron microscopy (SEM) is used to analyse the different microstructures. At 600°C, 2 hr of operating time, and 4weight% alumina additions, the highest sintering density and microhardness are found.

1. Introduction

No one can deny that applied sciences play an important role in different fields as reported before. [1-6] Aluminum metal matrix composites (AMMCs) have exceptional features such as low density, high specific strength, high toughness, strong wear as well as corrosion resistance, creep resistance, low coefficient of thermal expansion, and high specific stiffness and are broadly applied in vehicles, ship construction, military, aerospace, and mineral processing sectors.[7-10] AMMCs are manufactured utilizing a number of processes, and composite characteristics vary depending on the manufacturing conditions. Aluminum alloy composites have traditionally been produced using both solid-state processing (such as mechanical alloying, friction stir processing, and powder metallurgy) and liquid-state processing (compo-casting, stir casting, squeeze casting etc.). Powder metallurgy, as compared to other production processes, exhibits homogeneous particle distribution with no agglomeration, dendrite separation, or undesirable chemical reaction at the interface.[11-12] Powder Metallurgy (PM)allows for a significant deal of flexibility in altering the microstructure (for example, higher volume fraction, as well as different sizes and morphologies of particle reinforcement, may be utilized).[13-19]

Without incurring machining expenses, PM can mass-produce complicated and accurate items in near-net form.[20] To achieve the appropriate microstructure and increase mechanical characteristics, all particles in the matrix must be dispersed evenly.[12] However, because of their low wettability in the metal matrix and high surface-to-volume ratio, achieving homogeneous distribution of tiny ceramic particles in the metal matrix is a significant difficulty. Ceramic particle reinforced metal matrix composites (PMMCs) are now gaining popularity due to their low cost, isotropic characteristics, and simplicity of manufacture.[21-22] Many researchers used different ceramic particle reinforcements such as Al_2O_3, SiC, TiB_2, B_4C, Si_3N_4, ZrB_2, AlN, TiC, and WC in particulate metal matrix composites to increase attributes such as micro hardness, corrosion resistance, wear resistance, and the high strength-to-weight ratio.[23-28]

* Corresponding author. Fax-+91 - 674 - 2350642
 E-mail address jajneswarnanda@soa.ac.in (J. Nanda)

Al_2O_3 is the another most common ceramic reinforcement used in AMMCs after SiC, and it is one of the most firmly bound compounds with aluminum.[29]It possesses a high ionic interatomic bonding force that contributes to the wear resistance and compressive strength of the aluminum alloy to which it was added .[30]Along with many other objects, Al_2O_3 is used to manufacture connecting rods, piston rings, diesel engine pistons, drive shafts, braking discs, and cylinder liners.[31]Several authors used powder metallurgy to create AMMCs with Al_2O_3 reinforcement and found that the presence of alumina enhanced compressive strength and hardness.[32-33] Alumina has a high hardness, specific strength, mechanical performance, chemical stability, and high-temperature properties, making it appropriate for use as a refractory material, abrasive, and coating.[28, 34]Vogel et al.[35]recently explored the influence of alumina concentration and shape on the mechanical characteristics of bulk nano-laminated Al_2O_3 composites.

Compacting pressure, sintering duration, sintering temperature, and reinforcing proportion are key process parameters that influence the characteristics of powder metallurgy composites.[32]Rohatgi et al[36] investigated the tribological characteristics of AMMCs reinforced by graphene Nano platelets produced by a powder metallurgy technique and revealed that process parameters had a substantial impact on mechanical and wear performances. According to Bains et al.[37], the parameters connected with the PM approach for the manufacture of metal matrix composites (MMCs) had a more noticeable influence on mechanical characteristics as well as homogenization. Vani and Chak[32] conducted a study on the effect of process parameters, such as compaction pressure, sintering temperature, and time, on the characteristics of composites. They revealed that by optimizing these process parameters, it is possible to accomplish homogeneous reinforcement distribution in the matrix that improves composite mechanical properties. Several authors have used various binders in their works. Among them are zinc stearate (Zn $[C_{18}H_{35}O_2]$), stearic acid ($C_{18}H_{36}O_2$), and Acrawax 'C' ($C_{38}H_{76}N_2O_2$). Zinc stearate has a substantial effect on sintering density whereas Acrawax 'C' has a slight effect on the modification of density during solid state sintering. During heating, zinc stearate decomposes into ZnO. Because of its high melting point of around 1950°C, Zn remains in the powder compact up to the sintering temperature and consequently remains in grain boundaries or closed pores. The pressure within the pores having Zn residues gradually increases and causes substantial stress in the matrix, resulting in significant swelling and a decrease in density.[38] Powder metallurgy was used to manufacture alumina based AMMCs in this study.

The novelty of this work are as follows:
1. In the present article, the simultaneous impact of compaction pressure as well as various combinations of sintering temperature and sintering time with weight percent of alumina on the physical, structural, and mechanical characteristics of the Al-alumina composite was analysed. From the literature, it was found that in most of the work, the researchers have considered any two of the above parameters (compaction pressure, sintering temperature, sintering time, and weight percentage of alumina) in their investigations.[39]
2. Acrawax 'C' ($C_{38}H_{76}N_2O_2$) was used as the binder in the preparation of the composite instead of zinc stearate (Zn $[C_{18}H_{35}O_2]$) or stearic acid ($C_{18}H_{36}O_2$) which were in use by most of the researchers in their investigation.[39]

2. Results and Discussion

2.1 Compacting Pressure Determination

Both green and sintered composites indicated a nominal difference in density for aluminum with 8wt% Alumina after 55kN (486MPa) of compacting pressure. However, there was a substantial increase in wear and strain in the die-punch assembly. A similar experiment was conducted with varied alumina percentages from 2% to 6%. Finally, all the above alumina compositions need compacting pressures lower than 486 MPa. Therefore, the load of 486 MPa is taken as the compacting pressure for the whole experiment. This method of selecting compacting pressure has also been published in the literature.[20] **Fig.1** illustrates a compacting pressure vs. density curve for Al-8wt% Alumina (both green and sintered).
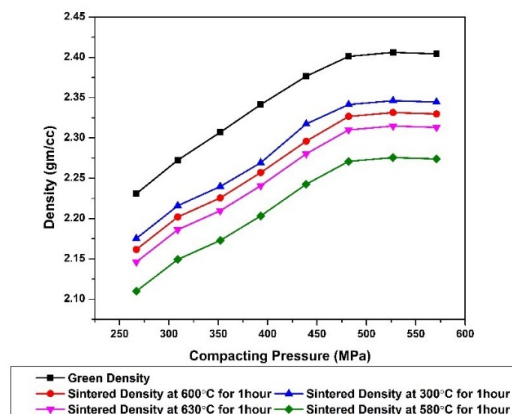

Fig. 1. Variation of density with compacting pressure for Al-8wt% Alumina

2.2 Density and Porosity Measurement

The densities of sintered samples were determined by means of the Archimedes principle, and the porosity percentage was computed using sintered density and theoretical density. The sintered density was computed using the correlation shown below (Equation 1).

$$\rho_s = \left[\frac{m_a}{m_a - m_w} \right] \times \rho_w$$

(1)

m_a and m_w are the mass of component in air and in water respectively. ρ_w (0.998g/cc) is the density of water at room temperature.

2.2.1 Effect of Sintering Temperature on sintering density and porosity

The diffusion phenomenon affects the sintering density. Higher sintering temperatures cause more diffusion and, as a result, a denser and less porous structure.[40] As the sintering temperature rises, the atoms migrate very swiftly. It causes strong particle necking, resulting in a denser and pore-free microstructure.[41] The diffusion rate increases with temperature, resulting in higher material diffusion in the pores at elevated temperature.[42] However, at high temperatures, the material undergoes thermal expansion as well as grain growth. Grain growth and diffusion are two contrasting phenomena: diffusion increases the density and strength of composite whole grain growth reduces the same. Diffusion mechanisms prevailed over thermal expansion in the material, resulting in a rise in density. [41, 43, 44, and 45] **Fig. 2(a) to 2(f)** show the effect of sintering temperature on the sintering density and porosity of Al-alumina composites with varying quantities of alumina. The overall maximum sintering density (2.38829 gm/cc) was discovered at T=600°C for 4wt % alumina after 2 hours of sintering. At higher temperatures, the sintering density of composites decreased for all compositions and durations based on factors including grain growth, thermal expansion, and increased porosity.[43-45] In the current study, increasing the sintering temperature (up to 600°C) causes a rise in density and a decrease in porosity due to the superiority of diffusion over thermal expansion and grain growth, but increasing the temperature further (630°C and higher) causes the opposite, i.e., density declines and porosity rises due to the superiority of thermal expansion and grain growth over diffusion. [44, 46, 47]

2.2.2 Effect of Sintering time on sintering density and porosity

Diffusion is affected not just by temperature but also by time. Thus, sintering time has a substantial impact on density. The relationship between diffusion and sintering time helps to understand these phenomena. It is established that the atomic displacement is proportional to the square root of the sintering time. This promotes atom diffusion, culminating in coarse grains and a reduction in sintering density.[41, 43, 44, and 45] Atomic diffusion is a function of both temperature and time, and under the right conditions, homogenization and grain movement can occur. Temperature and time have a direct relationship to grain growth. Sintering duration, like sintering temperature, has a mixed impact, since increasing time causes both diffusion and grain development.[48] **Fig. 3 (a) to 3 (f)** represent the variation of sintering density and porosity with sintering time. After 2 hours of sintering at 600 °C and 4% alumina, the total maximum sintering density (2.38829 gm/cc) was observed. The effects of grain growth, thermal expansion, and increased porosity reduced the sintering density of composites for each composition. In the present analysis, with a rise in sintering time (up to 2hr); there is a rise in density and a decrease in porosity owing to the domination of diffusion over thermal expansion and grain growth. However, as time proceed on (2.5 hr. and later), the density falls and the porosity rises due to the prominence of thermal expansion and grain growth over diffusion.[46]

2.2.3 Effect of alumina weight percentage on sintering density and porosity

Alumina has an important role in sintering density. The composite's sintering density is increased (up to 4 wt. percent alumina content) before decreasing. As a result, porosity reduces to 4 wt.% alumina and rises further. This is due to uneven dispersion of alumina powder in the composite. Further agglomeration and interparticle friction both prevent particle rearrangement. Uniform alumina dispersal and embedding are limited to the addition of 4 wt. percent alumina due to alumina particle agglomeration. The agglomerated alumina restricted the contact area between the aluminum particles, limiting particle rearrangement and preventing alumina from being adequately absorbed into aluminum powders.[41]

Fig. 2(a), 2(c), and 2(e) illustrate sintered density as a function of sintering temperature for various alumina percentages with sintering timeframes (1.5, 2, and 2.5 hr., respectively). **Fig. 2(b), 2(d), and 2(f)** reveal the correlation between porosity and sintering temperature for various alumina percentages and sintering times (1.5, 2, and 2.5 hr., respectively).
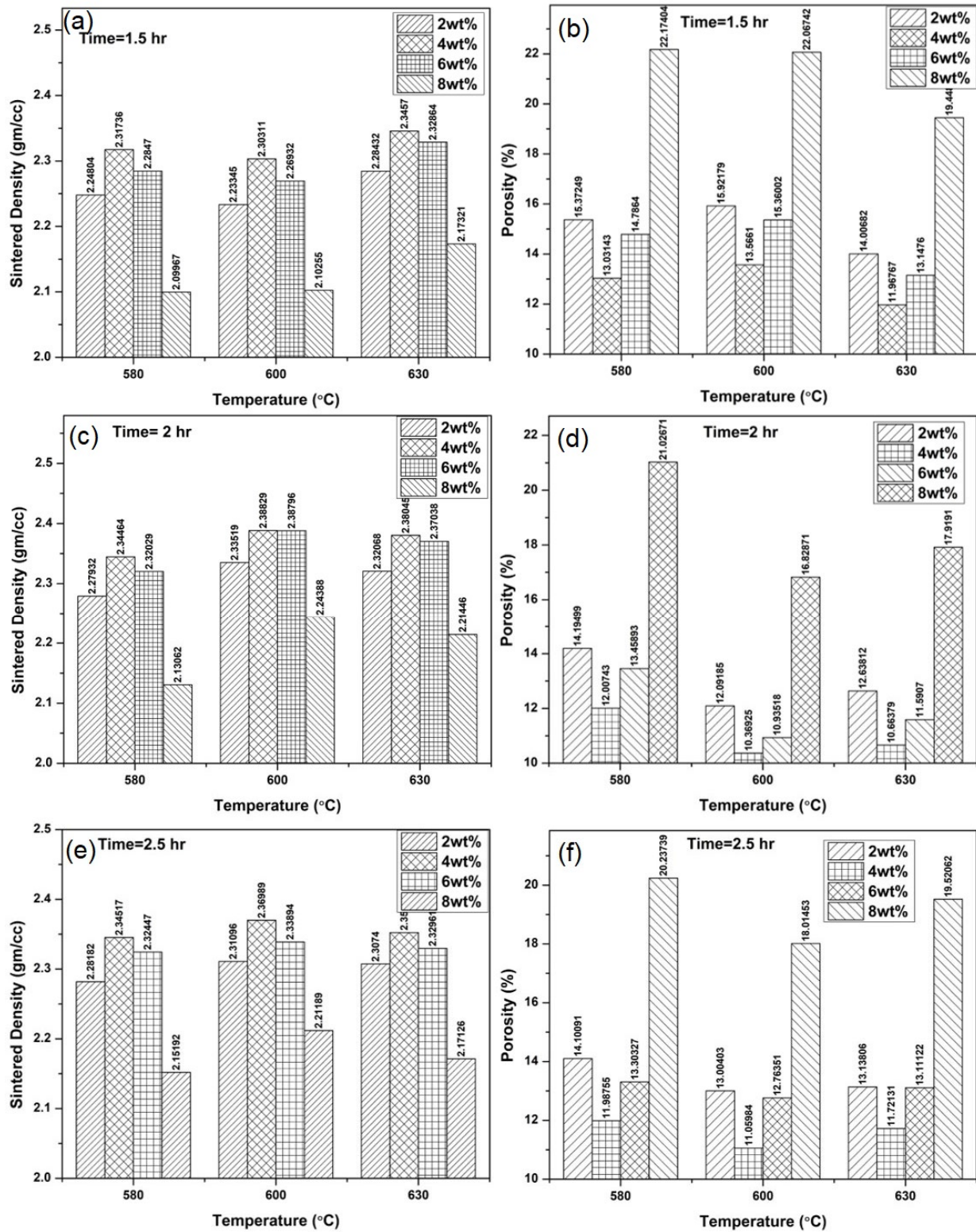
Fig. 2. (a), (c), (e)Variation of sintering density with sintering Temperature at various alumina wt.% **Fig. 2. (b), (d), (f)** Variation of Porosity with sintering Temperature at various alumina wt.%
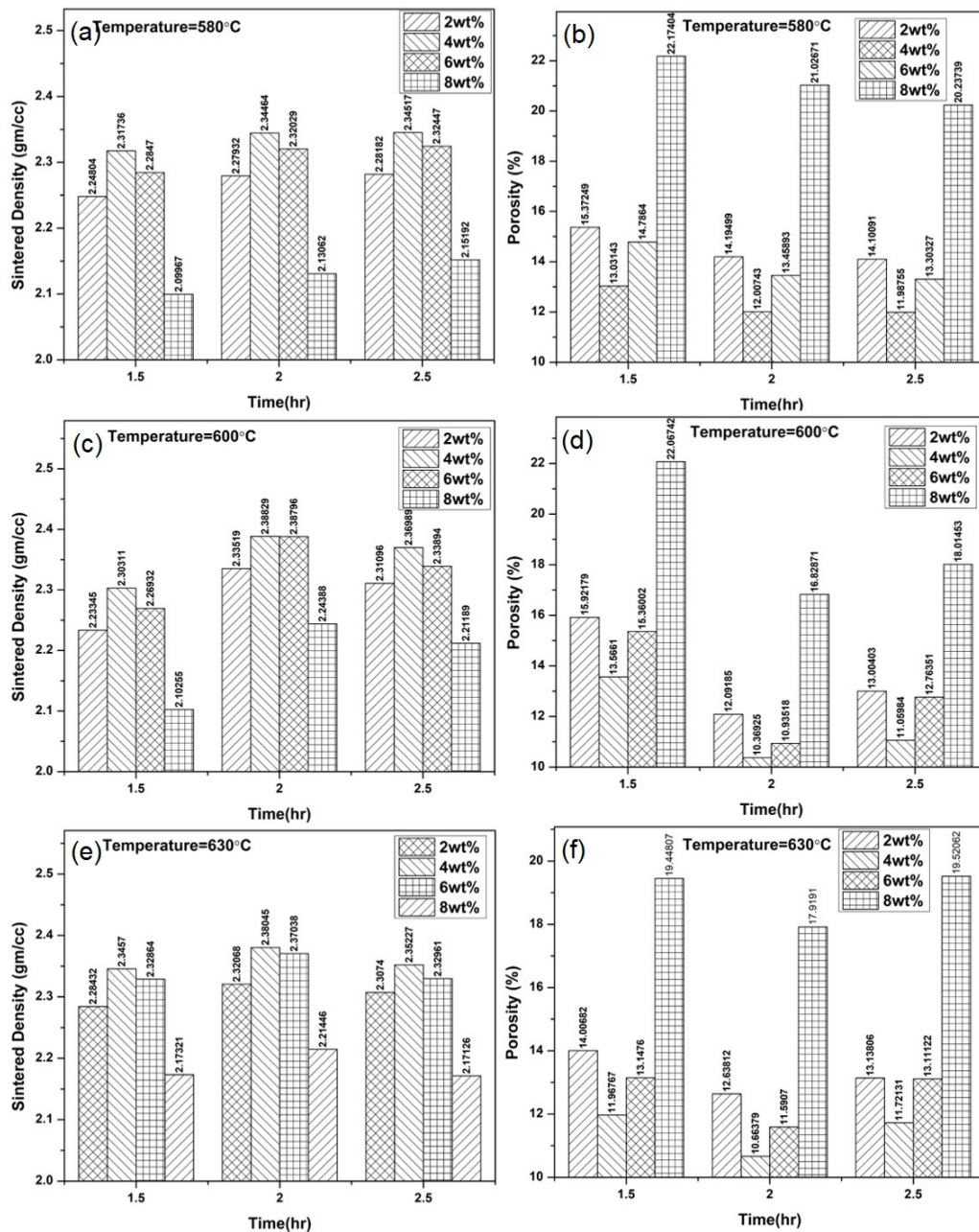
Fig. 3. (a), (c), (e) Variation of sintering density with sintering Time at various alumina wt.% **Fig. 3. (b), (d), (f)** Variation of Porosity with sintering Time at various alumina wt.%

Sintered density vs. sintering time for different alumina percentages at different sintering temperatures (580°C, 600°C, and 630°C, respectively) are presented in **Fig. 3(a), 3(c), and 3(e). Fig. 3(b), 3(d), and 3(f)** show porosity versus sintering time for various sintering temperatures (580°C, 600°C, and 630°C, respectively) with alumina percentages.

2.3 Hardness of composite sample

The hardness of a material can be used to predict its tensile strength, ductility, wear resistance, and other physical properties. The hardness values are computed using the indent created on the sample surface.

2.3.1 Influence of sintering time, temperature and alumina addition on Hardness

Hardness is altered not just by high sintering temperatures, but also by the period of time the test specimen is subjected. Because of appropriate material diffusion in the pores, strong diffusion bonding among the particles, decreased porosity, and higher density, hardness rises with increasing sintering temperature and time (up to a limit).[18,49] However, it has been observed that increasing the temperature and time reduces the hardness, with a rise in sintering temperature and time contributing to grain development and porosity.[18,46] The hardness of Al-alumina composites is shown in **Fig. 4(a) and 4(b)**

as a function of sintering time, temperature, and alumina content. The composites are sintered at three different temperatures: 580°C, 600°C, and 630°C, for 1.5 hr., 2 hr., and 2.5 hr. The optimum sintering temperature was observed to be 600°C, where the highest value of hardness (57 HV) is obtained at t = 2 hr. for 4 wt. percent alumina content.

In this sintering temperature analysis (as shown in **Fig. 4a**), increasing the temperature of the specimen to a high temperature (up to 600°C) lead to a rise in hardness, but increasing the exposure temperature of the specimen (630°C and later) resulted in a decrease in hardness. Because of the decreased porosity, a densified and more closely bound microstructure may be recognized at a higher sintering temperature, resulting in high hardness. Higher temperatures, on the other hand, provoke grain growth and a loss of hardness.[44]This pattern of rising and decreasing hardness is also presented in literature.[40]

The sintering time analysis is presented in **Fig. 4b**. The hardness of the specimen was found to rise when the exposure duration was increased to 2 hr., while it was found to decrease when the exposure time was increased to 2.5 hr. This is due to atom diffusion, which induces a decrease in pore volume, resulting in greater hardness, however, after a critical point, coarse grains are generated with increasing time. As a result, bigger grain sizes of aluminum decrease the hardness of AMMC composites. The influence of sintering duration on mechanical characteristics is presented in literature.[44]

The weight % of reinforcement is also a decisive aspect in the hardness of AMMC. Composites with uniformly disseminated alumina and completely bound particles are stronger. In achieving good particle bonding without grain growth, alumina content is an important factor in MMC. It is observed that the addition of alumina up to 4wt% increases the hardness as shown in **Fig. 4a and 4b**. But further addition of alumina to the composite results in a decreasing trend of hardness. Alumina content is a critical component in MMC for obtaining effective particle bonding without grain development. As indicated in **Fig. 4a and 4b**, the addition of alumina up to 4wt percent enhances the hardness. However, adding more alumina to the composite resulted in a declining hardness trend. This improvement in hardness at 4% alumina addition is due to the reduction of dislocation movement during plastic deformation, which increases the interface area between aluminum and alumina particles and inhibits grain development during sintering.[43-45] The inclusion of reinforcement after 4% reduces hardness due to alumina agglomeration.[50-51] Friction among particles is produced by these agglomerated powders, i.e., suppressing the interaction between Al and alumina, resulting in a weak interface between the particles that increases porosity and a decline in micro-hardness.
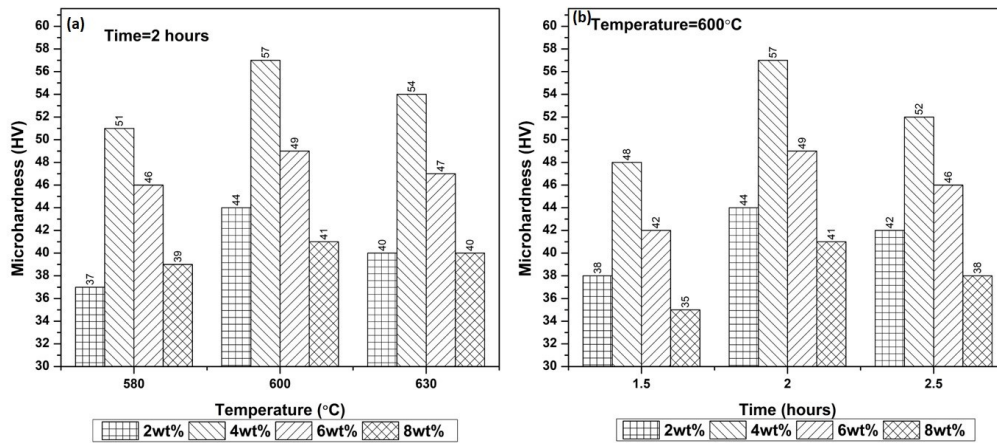

Fig. 4.a Average Micro-Hardness (HV) vs sintering temperatures for 2hr at various alumina weight%. **Fig. 4.b** Average Micro-Hardness (HV) vs sintering time for 600°C at various alumina weight%

2.4 Structural and Morphological Study

Fig. 5 exhibits XRD plots of alumina, pure aluminum, and composites synthesized at 600°C and 2 hours (for the optimum hardness and sintering density). The XRD of alumina shows the presence of various alumina structures like α-alumina (00-42-1468), γ-alumina (00-29-0063), κ-alumina (00-88-0107), θ-alumina (00-35-0121), and δ-alumina (00-88-1609). According to the XRD plots of composites, five significant peaks at 2θ of 39.079° (111), 45.86° (200), 65.74° (220), 78.78° (311), and 82.98° (222) belongs to aluminium with JCPDS card number (00-001-1180). The other significant peak found at 2θ of 31.0157° is attributed to alumina (004) with JCPDS card number (00-35-0121). The purity of composites is evident from their XRD patterns, as no other phases other than Al and Al_2O_3 are found. The crystallite size of composites was calculated using the Williamson-Hall plot[52] which is depicted by equation 2 as follows:

$$\beta \cos\theta = 4\varepsilon \sin\theta + \frac{K\lambda}{D} \tag{2}$$

where θ is the peak angle, β is the FWHM (full width half maximum) value, K= shape factor (0.9), Ɛ=residual strain, λ= wave length of CuKα radiation, and D= crystallite size. Equation (2) can be compared with a straight-line equation, y=mx+ c. Where, m= slope and c= intercept. A plot of βCosθ versus 4Sinθ known as the Williamson–Hall plot represents the average crystallite size (from the intercept) component and the average strain (from the slope) component. **Table 1** presents the crystallite size of composites. **Fig. 6** presents the linear fit of data (βCosθ vs. 4Sinθ) for various composites.
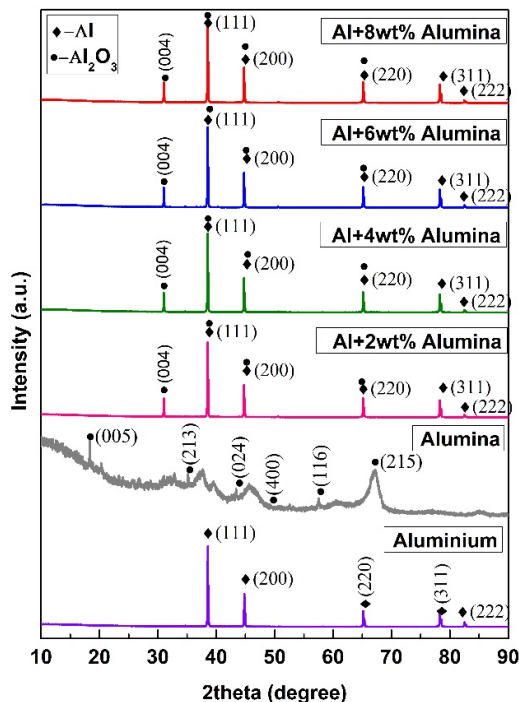

Fig. 5. XRD analysis of aluminium, alumina and composites at best sintering time (2hr) and best sintering temperature (600°C)

Table.1. Crystallite size of composites

Sample	Intercept (Kλ/D)	Crystallite Size(D)(nm)
Pure Al	0.000975	142.2092307
Al+2wt% Alumina	0.000836213	165.8118207
Al+4wt% Alumina	0.00094256	147.1036327
Al+6wt% Alumina	0.000708036	195.8290256
Al+8wt% Alumina	0.00058775	235.9064228

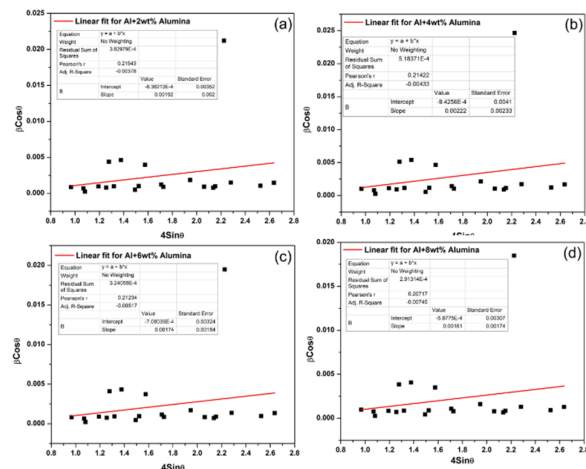**Fig. 6**. Linear fit of datas (βCosθ Vs 4Sinθ) for (a) Al-2wt% alumina (b) Al-4wt% alumina (c) Al-6wt% alumina (d) Al-8wt% alumina

2.5 Microstructure analysis

Fig. 7((a)-(d)) show the effect of alumina content on the microstructure of Al-2wt% alumina, Al-4wt% alumina, Al-6wt% alumina and Al-8wt% alumina composites at their best sintering temperature (600 °C) and time (2 hr). The figure represents how the microstructure of the composites alters as the alumina content increases. Pores are observed to be abundant at 2wt percent alumina addition, resulting in lower density and hardness with high porosity. The SEM reveals strong bonding between alumina-aluminum particles at 4wt% alumina addition, which is substantiated by the maximum sintering density and hardness. The presence of hard particles (alumina) near the grain boundaries, as well as excellent neck forms among the aluminum particles, improves the material's hardness. The micrograph shows a higher number of pores as the alumina percentage increases (at 6 and 8wt percent alumina), indicating poor interfacial bonding between reinforcement and matrix that results in a decline in mechanical characteristics such as hardness.

Alumina particles, through a dispersion strengthening process, limit the migration of dislocations in pure aluminum. Raising the alumina concentration to 4wt% decreased the gap between the reinforcing alumina particles as observed in the microstructure. Reduced spacing between alumina particles increases the required stress for dislocation migration, resulting in enhanced material strength.

When the alumina content exceeds 4 wt.%, the number of pores rises, thus the sintering density and hardness decrease. Increased alumina content increases the possibility of clustering and induces the formation of weak spots in the material, as shown in the microstructure of composites, reducing the hardness. [41, 43, 44 and 45]
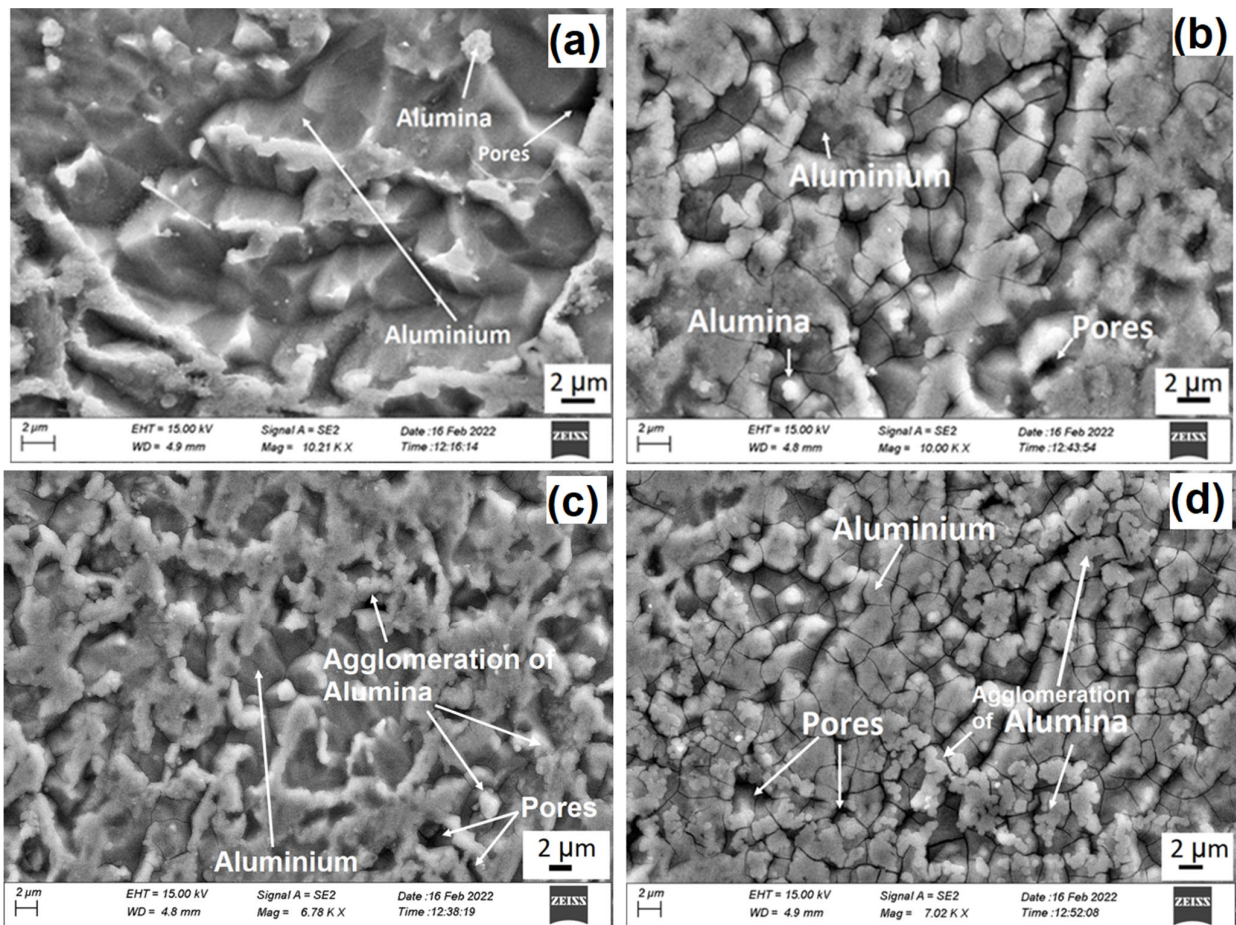
Fig. 7. (a) Microstructures of Al-2wt% alumina, **(b)** Al-4wt% alumina and **(c)** Al-6wt% alumina **(d)** Al-8wt% alumina at optimum temperature (600°C) and time (2hr)

3. Conclusions

The current study presents a complete characterization of the sintered density, porosity, structural (XRD), and mechanical characteristics (hardness) of Al_2O_3 dispersed Al-based composites as compacting pressure, sintering time, temperature, and Al_2O_3 content vary. The aforesaid study yielded the following findings.

The compacting pressure of 486 MPa (55KN of compacting load) is chosen to fabricate the composite since increasing the load produces no substantial change in density but causes wear and tear of the die-punch assembly. The optimal sintering temperature and duration for highest sintering density and maximum micro-hardness are found to be 600 °C and 2 hours, respectively.

Sintering density and micro-hardness are found to be highest when 4wt% alumina is added to the aluminum matrix. At 4wt% alumina addition into the aluminum matrix, the porosity is minimized. The structural analysis (XRD) reveals that the reinforcing phase preserves its structure with no substantial alteration. The SEM data correlate well with the experimental results.

The synthesised composites can find application in light-weight, hard, and abrasion/wear-resistant materials. The future direction of this study is to fabricate low-cost but highly reliable and environment-friendly composites by adding bio-wastes to these present composites and analysing their behaviour in different processing conditions.

4. Experimental

4.1. Materials

Aluminum-alumina (2, 4, 6, and 8wt %) composites were manufactured by means of the conventional powder metallurgy technique. To fabricate the composite, pure aluminum powder with average particle size of 63μm was used as the matrix with Al_2O_3 reinforcement of the same particle size. **Table 2** outlines both the matrix and the reinforcement phase.

Table. 2. Details of constituents

Powder Material	Weight Percentage	Average Particle Size(μm)	Density(g/cm^3)
Al	96,94,92,90	63	2.7
Al_2O_3	2,4,6,8	63	3.95
Binder	2	-	0.97

The chemical compositions of aluminum and alumina were determined by XRF analysis on a Bruker XRF Alloy analyzer, as shown in **Tables 3** and **4**.

Table. 3. Chemical composition of Aluminum

Compound formula	Al	Fe_2O_3	SiO_2	Ga_2O_3	As_2O_3	Others
Percentage	99.0566	0.291	0.212	0.108	0.106	%Uncounted weight

Table. 4. Chemical composition of Alumina

Compound formula	Al_2O_3	SiO_2	Na_2O	Cl	Fe_2O_3	SO_3	BaO	MgO	K_2O	Others
Percentage	94.521	1.890	1.444	1.184	0.163	0.151	0.125	0.125	0.101	%Uncounted weight

4.2. Methods

The three key steps in the powder metallurgy method are mixing or blending, powder compaction, and sintering. Initially, a predetermined quantity of pure aluminum with alumina powder of same size (63μm) is added up with Acrawax'C' as binder (according to the composite's composition) with a digital microbalance.

To achieve a homogeneous dispersion of Al_2O_3, the mashed powder is put through a high-speed horizontal ball milling machine for 30 minutes. The slurry was then poured into an EN-24 steel die. The die walls were lubricated with zinc stearate. Green compacts of cylindrical specimen with 12mm diameter and 30mm length (ASTM G99-05 standard) were manufactured using a FIE Universal Testing Machine (UTM) under a compacting load of 30 KN-65 KN with rising by 5 KN to accurately assess the optimal compacting pressure of green composite, and the mass of each specimen was maintained constant. All specimens were sintered in the tube furnace under vacuum conditions at different sintering temperatures (580°C, 600°C, and 630°C) at durations (1.5hr, 2 hr., and 2.5 hr.). The density of the sample was calculated using Archimedes' Principle and the theoretical density was obtained using the rule of mixture. An X-ray diffractometer was used to perform XRD analysis to determine the phase (Rigaku rent 2200). SEM (JEOL JSM – 7001F) was utilized to examine the microstructure of composites. The sintered composites' micro-hardness was determined by using a Vickers micro-hardness tester with a weight of 0.025Kg and indentation duration of 15s.

314

References

1. Saber A. F., Sayed M., Tolba M. S., Kamal El-Dean A. M., Hassanien R., and Ahmed M. (**2021**) A facile method for preparation and evaluation of the antimicrobial efficiency of various heterocycles containing thieno [2, 3-d] pyrimidine. *Synth. Commun.*, 51(3) 398-409.
2. Kamal El-Dean A. M., Zaki R. M., Radwan S. M., and Saber A. F. (**2017**) Synthesis, reactions and spectral characterization of novel thieno pyrazole derivatives. Eur. Chem. Bull., 6(12) 550-553.
3. Zaki R. M., Kamal El-Dean A. M., Radwan S. M., and Saber A. F. (**2019**) Efficient synthesis, reactions and spectral characterization of pyrazolo [4',3':4,5] thieno[3,2-d] pyrimidines and related heterocycles. Heterocycl. Commun., 25(1) 39–46.
4. Zaki R. M., Kamal El-Dean A. M., Radwan S. M., and Saber A. F. (**2018**) A Convenient Synthesis, Reactions and Biological Activity of Some New 6H-Pyrazolo [4',3':4,5] thieno[3,2-d] [1,2,3] triazine Compounds as Antibacterial, Anti-Fungal and Anti-Inflammatory Agents. J. Braz. Chem. Soc., 29 (12) 2482-2495.
5. Saber A. F., Kamal El-Dean A. M., Redwan S. M., and Zaki R. M. (**2020**) Synthesis, spectroscopic characterization, and in vitro antimicrobial activity of fused pyrazolo [4′, 3′: 4, 5] thieno [3, 2-d] pyrimidine. J. Chin. Chem. Soc., 67(7) 1239-1246.
6. Abdelgalil A., Mustafa A.A., Ali S. A. M., and Yassin O. M. (**2022**) Effect of irrigation intervals and foliar spray of zinc and silicon treatments on maize growth and yield components of maize. Curr. Chem. Lett., 11(2) 219–226.
7. Taha M.A. (**2001**) Industrialization of cast aluminum matrix composites (AMMCs). *Mater. Manuf. Process*,16(5) 619–641.
8. Kim C.S., Cho K., Manjili M.H., and Nezafati M. (**2017**) Mechanical performance of particulate reinforced Al metal-matrix composites (MMCs) and Al Metal-Matrix Nano-Composites (MMNCs). *J. Mater. Sci.,* 52(23) 13319–13349.
9. Anthony M., Schultz B.F., Rohatgi P.K., and Gupta N. (**2014**) Metal matrix composites for automotive applications. in: Elmarakbi A. (Ed) Advanced Composite Materials for Automotive Applications: Structural Integrity and Crashworthiness. John Wiley & Sons, UK, 313-344.
10. Bhoi N.K., Singh H., and Pratap S. J. (**2020**) Developments in the aluminum metal matrix composites reinforced by micro/nano particles – a review. Compos. *Mater.,* 54(6) 813–833.
11. Harris S.J. (**1990**) Developments in Particulate and Short Fiber Composites. AGARD Lectures Series no. 174, New Light Alloys, 4:1-4:21.
12. Prabhu B., Suryanarayana C., An L., and Vaidyanathan R. (**2006**) Synthesis and characterization of high-volume fraction Al–Al$_2$O$_3$ nanocomposite powders by high-energy milling. *Mater. Sci. Eng. A,* 425(1-2) 192-200.
13. Kainer K.U. (**2006**) *Metal Matrix Composites. Custom-made Materials for Automotive and Aerospace Engineering,* Wiley–VCH, Weinheim.
14. Miracle D.B. (**2005**) Metal matrix composites—from science to technological significance. *Comp. Sci. Technol.,* 65(15-16) 2526–2540.
15. Slipenyuk A., Kuprin V., Milman Y., Goncharuk V., and Eckert J. (**2006**) Properties of P/M processed particle reinforced metal matrix composites specified by reinforcement concentration and matrix-to-reinforcement particle size ratio. *Acta. Mater.,* 54(1) 157-166.
16. Alahelisten A., Bergman F., Olsson M., and Hogmark S. (**1993**) On the wear of aluminum and magnesium metal matrix composites. *Wear,* 165(2) 221–226.
17. Guo R.Q., and Rohatgi P.K. (**1996**) Compacting characteristics of aluminum–fly ash powder mixtures. *J. Mater. Sci.,* 31(20) 5513–5519.
18. Guo R.Q., and Rohatgi P.K. (**1997**) Preparation of aluminum–fly ash particulate composite by powder metallurgy technique. *J. Mater. Sci.,* 32(5) 3971–3974.
19. Rohatgi P.K., Huang P., Guo R., Keshevaram B.N., and Golden D. (**1995**) Morphology and selected properties of fly ash. in: Malhotra V.M. (Ed) Proceedings of the 5th CANMET/ACI International Conference on Fly Ash Silica Fume Slag and Natural Pozzolans in Concrete. American Concrete Institute, Detroit, MI, 459–478.
20. Judge W.D., Bishop D.P., and Kipouros G.J. (**2017**) Industrial Sintering Response and Microstructural Characterization of Aluminum Powder Metallurgy Alloy Alumix 123. *Metallogr. Microstruct. Anal.,* 6(5) 375-382.
21. Rao J.B., Rao D.V., Murthy I.N., and Bhargava N.R.M.R. (**2012**) Mechanical properties and corrosion behavior of fly ash particles reinforced AA 2024 composites. *J. Compos. Mater.,* 46(12) 1393–1404.
22. Slipenyuk A., Kuprin V., Yu M., Spowart J.E., and Miracle D.B. (**2004**) The effect of matrix to reinforcement particle size ratio (PSR) on the microstructure and mechanical properties of a P/M processed AlCuMn/SiCp MMC. *Mater. Sci. Eng. A,* 381(1-2) 165-170.
23. Sardar S., Karmakar S.K., and Das D. (**2015**) Evaluation of Abrasive Wear Resistance of Al$_2$O$_3$/7075 Composite by Taguchi Experimental Design Technique. *Trans. Indian. Instit. Met.,* 71(8) 1847–1858.
24. Poria S., Sahoo P., and Sutradhar G. (**2016**) Tribological characterization of stir-cast aluminium-TiB$_2$ metal matrix composites. Silicon, 8(4) 591–599.
25. Soltani S., Khosroshahi R.A., Mousavian R.T., Jiang Z.Y., Boostani A.F., and Brabazon D. (**2017**) Stir casting process for manufacture of Al–SiC composites. *Rare. Met.,* 36(7) 581–590.
26. Verma A.S., Suman K., and Suri N.M. (**2015**) Corrosion behavior of aluminum base particulate metal matrix composites: a review. *Mater. Today Proc.*, 2(4-5) 2840–2851.

27. Abdizadeh H., and Baghchesara M.A. (**2017**) Optimized Parameters for Enhanced Properties in Al–B$_4$C Composite. *Arab J. Sci. Eng.,* 43(9) 4475–4485.

28. Samal P., Vundavilli P.R., Meher A., and Mahapatra M.M. (**2020**) Recent progress in aluminum metal matrix composites: A review on processing, mechanical and wear properties. *J. Manuf. Process*, 59 131–152.

29. Pilania G., Thijsse B.J., Hoagland R.G., Lazić I., Valone, S. M., and Liu X. Y. (**2014**) Revisiting the Al/Al$_2$O$_3$ interface: coherent interfaces and misfit accommodation. *Sci. Rep.,* 4(1) 1–9.

30. Iqbal A.K.M.A., and Nuruzzaman D.M. (**2016**) Effect of the reinforcement on the mechanical properties of aluminium matrix composite: a review. *Int. J. Appl. Eng. Res.*, 11(21) 10408–10413.

31. Vani V.V., and Chak S.K. (**2018**) The effect of process parameters in aluminum metal matrix composites with powder metallurgy. *Manuf. Rev.,* 5(7) 1–13.

32. Abouelmagd G. (**2004**) Hot deformation and wear resistance of P/M aluminium metal matrix composites. *J. Mater. Process. Technol.*, 155–156 1395–1401.

33. Gudlur P., Boczek A., Radovic M., and Muliana A. (**2014**) On characterizing the mechanical properties of aluminum-alumina composites. *Mater. Sci. Eng. A,* 590 352–359.

34. Chen W.H., Lin H.T., Nayak P.K., and Huang J.L. (**2014**) Material properties of tungsten carbide–alumina composites fabricated by spark plasma sintering. *Ceram. Inter.,* 40(9) 15007–15012.

35. Vogel T., Ma S., Liu Y., Guo Q., and Zhang D. (**2020**) Impact of alumina content and morphology on the mechanical properties of bulk nano laminated Al$_2$O$_3$-Al composites. *Compos. Commun.,* 22 100462 https://doi.org/10.1016/j.coco.2020.100462

36. Khorshid M.T., Omrani E., Menezes P.L., and Rohatgi P.K. (**2016**) Tribological performance of self-lubricating aluminum matrix nanocomposites: role of graphene nanoplatelets. *Eng. Sci. Technol. Int. J.*, 19(1) 463–469.

37. Bains P.S., Sidhu S.S., and Payal H.S. (**2016**) Fabrication and machining of metal matrix composites: a review. *Mater. Manuf. Process,* 31(5) 553–573.

38. Kim S., Joung C., Kim H., Na S.H., Lee Y., and Sohn D. (**2002**) Resintering Behavior in Oxidatively Sintered UO$_2$ and UO$_2$-5wt%CeO$_2$ Pellet. *J. Nucl. Sci. Technol.*, 39(sup3) 697-700.

39. Manik M. K., Shing M. B., and Vhagat V. (**2022**) Laboratory Investigation of Composite Made of Alumina Dispersed Aluminum Prepared by UTM Pressed Powder Metallurgy Method. In Smart Technologies for Energy, Environment and Sustainable Development, 1 761-781. Springer, Singapore.

40. German R.M. (**1996**) *Sintering theory and practice,* Wiley, New York.

41. Gurbuz M., and Mutuk T. (**2017**) Effect of process parameters on hardness and microstructure of graphene reinforced titanium composites. *Compos. Mater.*, 0(0) 1–9.

42. Dixit M., and Srivastava R. (**2019**) The effect of copper granules on interfacial bonding and properties of the copper-graphite composite prepared by flake powder metallurgy. *Adv. Powder. Technol.,* 30(12) 3067-3078.

43. Rahimian M., Ehsani N., Parvin N., and reza Baharvandi H. (**2009**) The effect of particle size, sintering temperature and sintering time on the properties of Al–Al$_2$O$_3$ composites, made by powder metallurgy. *J. Mater. Process Technol.,* 209(14) 5387–5393.

44. Gurbuz M., Can Senel M., and Koç E. (**2018**) The effect of sintering time, temperature, and graphene addition on the hardness and microstructure of aluminum composites. *J. Compos. Mater.,* 52(4) 553–563.

45. Rahimian M., Ehsani N., Parvin N., and Baharvandi H. R. (**2009**) The effect of sintering temperature and the amount of reinforcement on the properties of Al–Al$_2$O$_3$ composite. *Mater. Des.,* 30(8) 3333–3337.

46. Umasankar V. (**2014**) Experimental evaluation of the influence of processing parameters on the mechanical properties of SiC particle reinforced AA6061 aluminium alloy matrix composite by powder processing. *J. Alloys Compd.,* 582 380–386.

47. Tiwari S., Rajput P., and Srivastava S. (**2012**) Densification Behaviour in the Fabrication of Al-Fe Metal Matrix Composite Using Powder Metallurgy Route. *Int. sch. Res. Notices.,* 2012 https://doi.org/10.5402/2012/195654

48. Burke P., and Kipouros G.J. (**2011**) Development of Magnesium Powder Metallurgy AZ31 Alloy Using Commercially Available Powders. *High. Temp. Mater. Proc.,* 30 51–61.

49. Saboori A., Novara C., Pavese M., Badini C., Giorgis F., and Fino P. (**2017**) An Investigation on the Sinterability and the Compaction Behavior of Aluminum/Graphene Nanoplatelets (GNPs) Prepared by Powder Metallurgy. *J. Mater. Eng. Perform.,* 26(3) 993–999.

50. Ezatpour H. R., Torabi-Parizi M., and Sajjadi S. A. (**2013**) Microstructure and mechanical properties of extruded Al/Al$_2$O$_3$ composites fabricated by stir-casting process. Trans. Nonferrous Met. Soc. China, 23(5) 1262−1268.

51. Pournaderi S., and Akhlaghi F. (**2017**) Wear behaviour of Al6061-Al$_2$O$_3$ composites produced by in-situ powder metallurgy (IPM). Powder Technol., 313 184-190.

52. Mote V. D., Purushotham Y., and Dole B. N. (**2012**) Williamson-Hall analysis in estimation of lattice strain in nanometer-sized ZnO particles. J. Theor. Appl. Phys., 6(1) 1-8.

316